Cylindrical vector beams reveal radiationless anapole condition in a resonant state

Yudong Lu[1], Yi Xu[1,2]*, Xu Ouyang[1,2], Mingcong Xian[2], Yaoyu Cao[1], Kai Chen[1] and Xiangping Li[1]*

Nonscattering optical anapole condition is corresponding to the excitation of radiationless field distributions in open resonators, which offers new degrees of freedom for tailoring light-matter interaction. Conventional mechanisms for achieving such a condition relies on sophisticated manipulation of electromagnetic multipolar moments of all orders to guarantee superpositions of suppressed moment strengths at the same wavelength. In contrast, here we report on the excitation of optical radiationless anapole hidden in a resonant state of a Si nanoparticle utilizing a tightly focused radially polarized (RP) beam. The coexistence of magnetic resonant state and anapole condition at the same wavelength further enables the triggering of resonant state by a tightly focused azimuthally polarized (AP) beam whose corresponding electric multipole coefficient could be zero. As a result, high contrast inter-transition between radiationless anapole condition and ideal magnetic resonant scattering can be achieved experimentally in visible spectrum. The proposed mechanism is general which can be realized in different types of nanostructures. Our results showcase that the unique combination of structured light and structured Mie resonances could provide new degrees of freedom for tailoring light-matter interaction, which might shed new light on functional meta-optics.

Keywords: anapole; multipole decomposition; all-dielectric nanoparticles

Introduction

Optical scattering of a nanopaticle under the excitation of a plane wave is usually determined by its predominant electromagnetic multipole moment[1]. Such predominant multipole moment can even decide the electric or magnetic nature of the scattering in all-dielectric photonics[2]. Therefore, tailoring such a predominant electromagnetic multipole moment becomes an effective and unified way to manipulate optical scattering[3]. Many abnormal optical scattering phenomena have been proposed to enable new possibility and functionality in photonics[3]. The nonscattering electromagnetic state is one of the typical examples[4–20] [see these elaborated reviews in refs.[21–24] for details]. In contrast to the embedded eigenstates or bound state in the continuum which cannot be accessed by the excitation in the continuum[25], the so-called electromagnetic anapole condition provides a nonscattering condition sustained under the excitation of external field[5,26], which resembles a promising physical mechanism for tailoring light-matter interaction in a nonscattering manner[21–24,27]. It is generally perceived that such an anapole condition requires that all of the

[1]Guangdong Provincial Key Laboratory of Optical Fiber Sensing and Communications, Institute of Photonics Technology, Jinan University, Guangzhou 510632, China; [2]Department of Electronic Engineering, College of Information Science and Technology, Jinan University, Guangzhou 510632, China.

*Correspondence: Y Xu, E-mail: yi.xu@osamember.org; XP Li, E-mail: xiangpingli@jnu.edu.cn

induced electromagnetic multipole moments are suppressed at the same wavelength, resembling the canonical way of realizing the radiationless anapole condition[4–20]. In particular, the optical anapole condition corresponds to a pronounced minimum in the far-field scattering associated with highly confined electromagnetic near-field[6,28]. Such condition is quite challenge to meet since the degree of freedom for tailoring the induced electromagnetic multipolar moments of a nanoparticle is quite limited. Such a condition can also be readily fulfilled through structured light illumination[16] which generally extends the scopes of light-matter interaction from both fundamental science and application prospective, such as high numerical aperture (NA) focusing[29–31], optical computation[32], optical data storage[33], customized excitation of electromagnetic multipole resonances[17,33–40] and radiationless anapole condition[9,16,17], enhancement of optical nonlinearity[41,42], optical tweezers[43–45] and advanced metrology[46,47].

According to Mie theory, the total scattering power of a spherical nanoparticle excited by a plane wave is determined by both contributions of electric and magnetic multipole moments of different order n [1].

$$P_{\text{total}} = \frac{\pi |E_i|^2}{k\omega\mu_0} \sum_{n=1}^{\infty} (2n+1)(|a_n|^2 + |b_n|^2) , \qquad (1)$$

where E_i, k and ω are the amplitude, k-vector and angular frequency of the incident plane wave, respectively. There are numerous zeros of Mie scattering coefficients a_n and b_n, which are corresponding to zero contribution to the total scattering from the electromagnetic multipole moments of different orders[48]. It was suggested that the electromagnetic anapole condition could be interpreted as the destructive interference between toroidal moments and Cartesian electromagnetic multipole moments[4–7,14,21,49–51]. In general, the zero amplitude conditions of a_n and b_n are usually accompanied with other spectral overlapping electromagnetic multipole moments. As a result, such zero conditions of Mie scattering coefficients could be physically hidden in far-field scattering response. For example, zero $|a_1|$ can even coexist with the resonant magnetic dipole (MD) condition at the same frequency[48].

In this paper, we show that sophisticated tailoring of electromagnetic multipolar moments in nanoparticles is not essential for the realization of the anapole condition, which is different from previous efforts in realizing the anapole condition[4–19]. In particular, we experimentally demonstrate that the combination of tightly focused cylindrical vector beam (CVB) and structured Mie resonances can reveal the radiationless anapole condition which is overlapped in spectrum with a resonant state. More importantly, it subsequently enables reconfigurable optical scattering of a silicon nanoparticle with simple morphology, where the optical scattering of the nanoparticle at a specified wavelength can be switched from the radiationless anapole condition to the magnetic resonant scattering condition and vice versa, as shown in Fig. 1.

Mechanism and numerical results

The electric field of a focused CVB can be expressed in terms of the electric and magnetic multipole fields[52]:

$$E_f(r) = \sum_{l=1}^{\infty} \sum_{-l}^{l} \left[p_{El}^0 N_l^0(r) + p_{Ml}^0 M_l^0(r) \right] , \qquad (2)$$

where p_{El}^0 and p_{Ml}^0 are the strength of the electric and magnetic multipole components, N_l^0 and M_l^0 are the vector spherical harmonics related to the electric and magnetic multipole components, respectively. For a RP beam
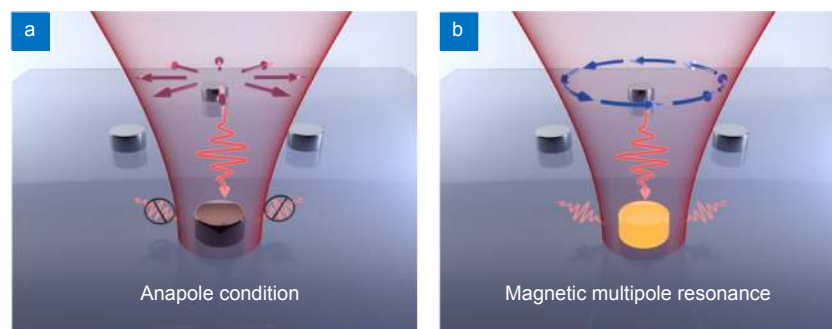

Fig. 1 | Schematic of a reconfigurable optical antenna which supports the radiationless anapole condition hidden in a magnetic resonances at the same frequency. Tightly focused RP (**a**) or AP (**b**) beam is used to selectively realize the nonscattering and resonant scattering scenarios of the optical antenna.

without orbital angular momentum, the magnetic component p_{Ml}^0 is zero while the electric component p_{El}^0 is zero for a AP beam[52]. As a result, the focused RP beam can be used to excite the electric and toroidal dipole moments because of their similarity of far-field radiation[9,16,39] while the focused AP beam can be used to excite the magnetic multipole modes[17,34−38]. As the excited strength of an electromagnetic multipolar mode depends on both the vectorial properties of the excitation source and the eigenmodes supported by the spherical nanoparticle, therefore, the key enablers for realizing high contrast reconfigurable optical scattering include two points: 1) a nanoparticle supports a pure electromagnetic multipole mode at a specified frequency, which is spectrally overlap with an anapole condition; 2) the spatial overlapping between the electromagnetic field of the nanoparticle's eigenmode and that of the tightly focused CVBs. High permittivity dielectric nanoparticles resemble a promising platform that fulfills both conditions. For a spherical Au core/Si shell nanoparticle (SN), the contributions of the spherical electric dipole (ED) can be designed to be totally suppressed at the resonant condition of MD[48]. One of the typical solution under plane wave excitation is shown in Fig. 2(a). If the scattering of a tightly focused AP beam is considered, it can be seen from Fig. 2(b) that all electric multipole moments have zero contribution to the total scattering, resembling the ideal MD scattering. On the contrary, the total scattering is zero at the same frequency of the MD resonance if the excitation of a tightly focused RP beam is applied, realizing the optical anapole condition, as shown in Fig. 2(c). Such a sharp contrast in optical scattering power of a nanoparticle at the same wavelength enables the realization of reconfigurable optical scattering.

In order to show the generality of this mechanism, we further consider a simple dielectric nanostructure where its magnetic quadrupole resonance overlaps with the anapole condition. Such dielectric nanostructure is much easier to fabricate in experiment than the core-shell nanoparticle. The Si nanodisk is optimized to fulfill the aforementioned enablers to realize high contrast reconfigurable optical scattering in the visible spectrum. According to the Cartesian electromagnetic multipole decomposition results under the excitation of a focused RP beam shown in Fig. 3(a), the destructive interference between the Cartesian ED and toroidal dipole moments results in the anapole condition where the contributions of high order electromagnetic multipole moments are
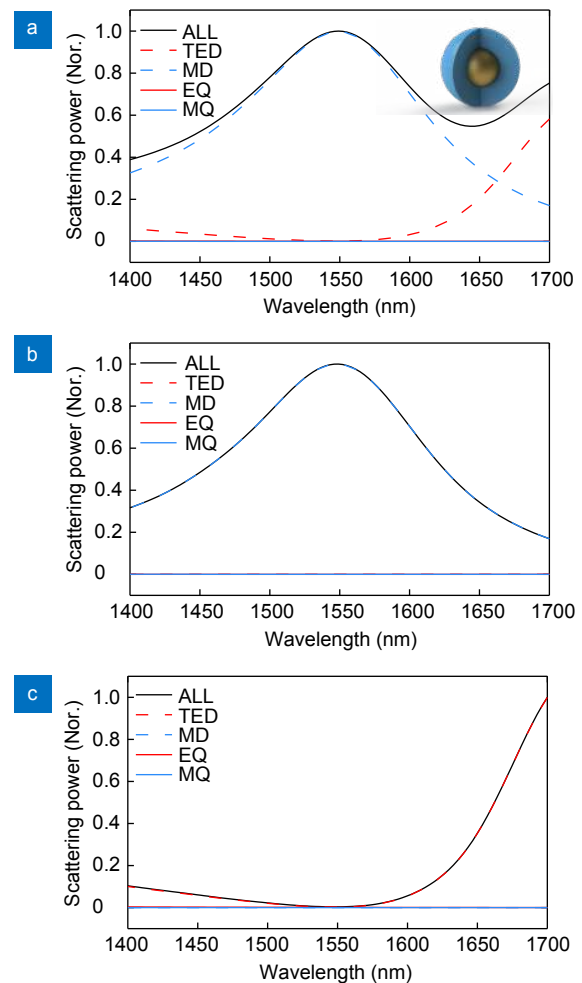
Fig. 2 | Numerical results of electromagnetic multipolar decomposition for the normalized scattering power of a Au core/Si shell nanoparticle under the excitation by (**a**) a plane wave, (**b**) a tightly focused AP beam and (**c**) a tightly focused RP beam. The radius of Au core is 86 nm while the outer radius of Si shell is 226 nm. The NA and magnification factor of the objective lens are 0.95 and 60, respectively. TED represents the contribution of toroidal and electric dipole to total scattering.

negligible. The schematic of current geometry (red) and the corresponding magnetic field (blue) are shown in the inset of Fig. 3(a). The calculated electromagnetic near-field distributions at different cross sections of the Si nanodisk are shown in Fig. 3(b) and 3(c) which manifest themselves as typical signatures of near-field excitation under the anapole condition[6]. If the excitation source is switched to a tightly focused AP beam, the Si nanodisk is turned into the resonant scattering condition, where the dominant Cartesian electromagnetic multipole is the electric quadrupole (EQ) moment. The corresponding electromagnetic near-field distributions are shown in Fig. 3(e) and 3(f), which validates qualitatively the dominant excitation of an MQ resonance. It should be
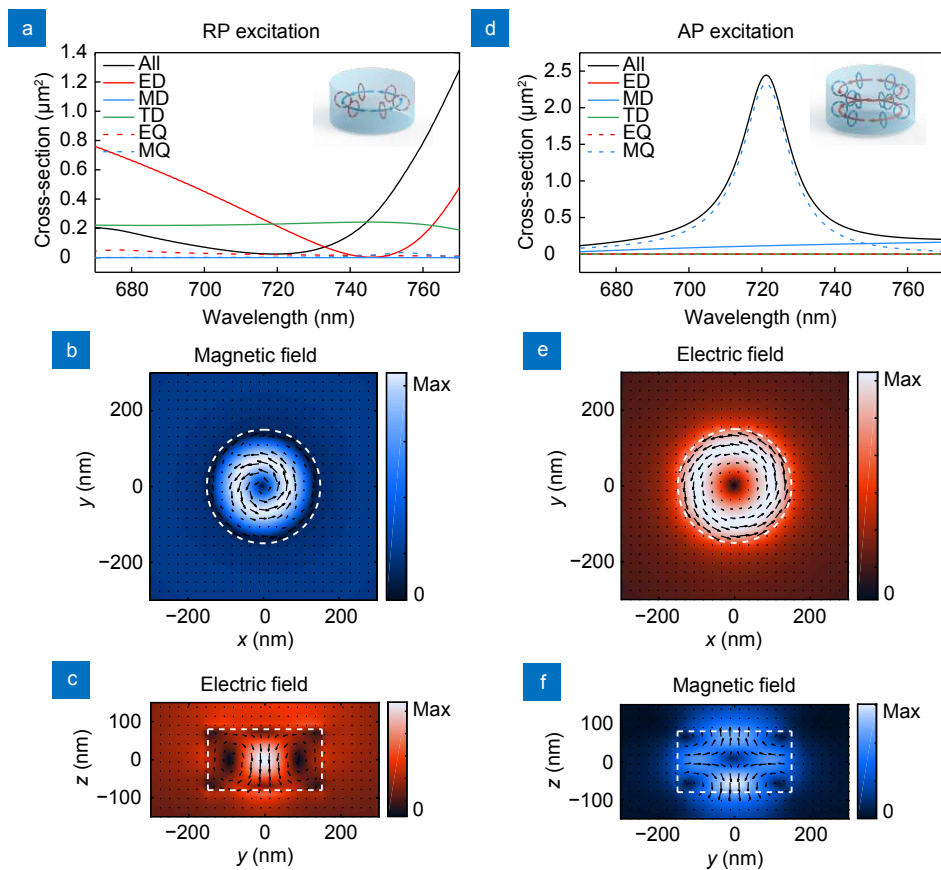
Fig. 3 | Cartesian electromagnetic multipolar decomposition results for the scattering power of a Si nanodisk under the excitation of (**a**) a tightly focused RP beam and (**d**) a tightly focused AP beam, respectively. Multipolar moments up to quadrupole are considered. The radius of Si nanodisk is r = 150 nm while its height is h = 160 nm. The corresponding electric and magnetic field distributions at several cross sections are shown in (**b**), (**c**) and (**e**), (**f**) under the anapole condition and magnetic quadrupole (MQ) resonance, respectively. All the wavelength are 720 nm. The NA and magnification factor of the objective lens are 0.95 and 60, respectively.

pointed out that there is still a residual induced MD moment accessed by the focused AP beam. More importantly, such high contrast reconfigurable optical scattering is tunable by simply changing the radius of the Si nanodisk, as shown in Fig. 4(a) and 4(b). As can be seen from this figure, the MQ resonance overlaps with the anapole condition quite well when the radius of the Si disk is changed. According to the calculated results of the Si nanodisk with different radius under the excitation of AP and RP beams, the wavelength of reconfigurable optical scattering can be effectively tuned about 50 nm, indicating sufficient tolerance for experimental demonstration.

Results and discussion

The Si nanodisk shown in Fig. 3 can be readily fabricated on a glass substrate (see Supplementary information Section 1). The substrate effect only has minor effect on the results of Fig. 3, as will be addressed in the

following. The geometry parameters of the Si nanodisk are outlined in Fig. 5(a), where the radius r of the Si nanodisk is 150 nm while the height h is 160 nm. The top and side views of scanning electron microscopy (SEM) images of the fabricated Si nanodisk are shown in Fig. 5(b) and 5(c), respectively. The side view is taken by tilting the sample stage of SEM by 30 degrees. As can be seen in Fig. 5(e), the back-scattering spectra measured by the home-built optical setup shown in Fig. 5(d) features a resonant scattering at around 735 nm under the excitation of tightly focused AP beam. The resonance wavelength is red-shifted compared with the result of Fig. 3(d) because of the substrate effect. However, the scattering intensity at the same wavelength is one order of magnitude smaller than the AP case when a tightly focused RP beam is used. This results quantitatively agree with the theoretical results of Fig. 3. The reason for small scattering signal collected at the anapole condition might be attributed to the morphology deformation (size
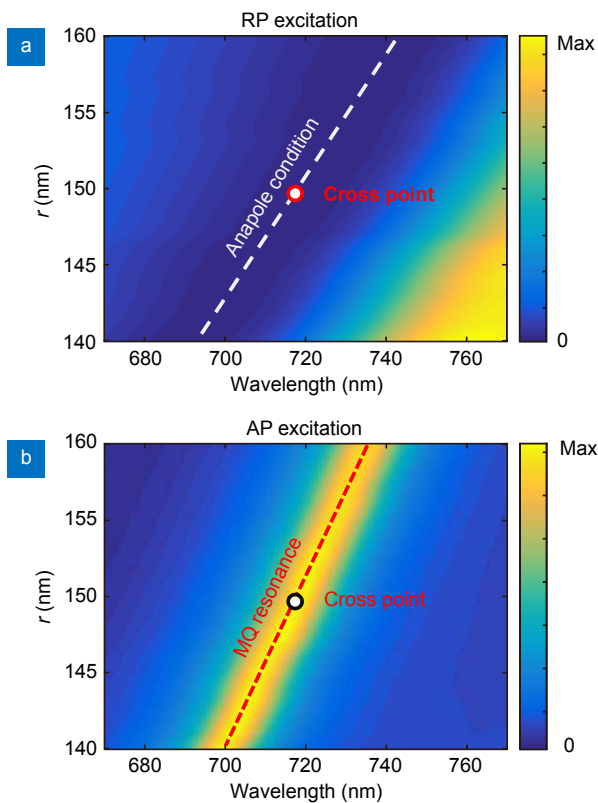
Fig. 4 | Evolution of the total scattering spectra for the Si nanodisk with different radius under the excitation of RP (**a**) and AP (**b**) beams with fixed focusing properties. The dependence of the anapole condition and MQ resonance on the radius of the Si nanodisk are outlined by dashed lines. The NA and magnification factor of the objective lens are 0.95 and 60, respectively.

difference and surface roughness) in the fabricated sample utilizing mask based inductively coupled plasma reactive ion etching (see Supplementary information Section 1), as shown in the inset of Fig. 5(b) and 5(c). In order to further access the scatteringless anapole condition, the preparation of Si nanodisks with well-defined morphology is subject to further optimization by e-beam lithography technology[6] and colloidal synthesis technology[16]. Furthermore, we can confirm from the dark-field back scattering images that the radiationless anapole condition is approached under the RP excitation [see Fig. 5(g)] while clear resonant scattering can be visualized in Fig. 5(f). These experimental results validate that the anapole condition can be realized without sophisticated tailoring of electromagnetic multipole moments of nanoparticle. More importantly, one can simply turn on or turn off the optical scattering of a fixed nanoparticle at the same wavelength utilizing tightly focused AP and RP beams, validating the concept of reconfigurable optical scattering for meta-optics. It is also expected that such a mechanism can be applied in the nonlinear scattering region, where distinct harmonic generation, stimulated Raman scattering and saturated scattering can be manipulated by different CVBs.

Conclusions

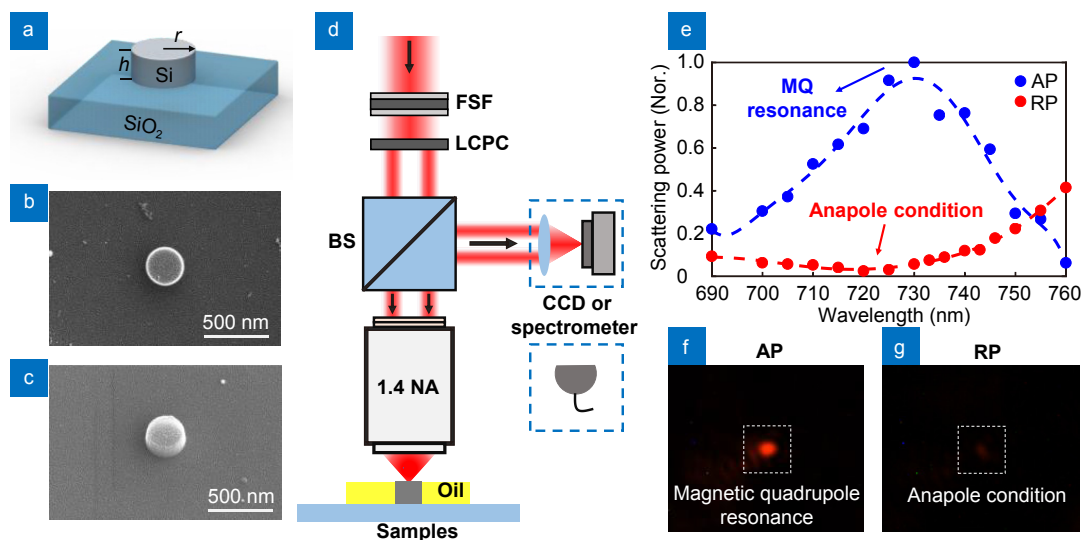In summary, we propose a new mechanism to excite the

Fig. 5 | (**a**) A Si nanodisk fabricated on a glass substrate, where h = 160 nm and r = 150 nm indicate its height and radius. SEM images of the Si nanodisk from top (**b**) and side (**c**) views. (**d**) Optical setup for the back scattering spectroscopy of CVBs. FSF, Fourier spatial filter; LCPC, liquid crystal polarization converter; BS, beam splitter; CCD, charge coupled device; NA, numerical aperture. (**e**) Experimental measured back scattering spectra of a Si nanodisk excited by AP (blue) and RP (red) beams under the same excitation power, respectively. The dashed lines are guide to the eye. CCD images under the MQ resonance condition excited by a focused AP (**f**) and the anapole condition excited by a focused RP (**g**). The excitation wavelengths for (f) and (g) are both 735 nm.

radiationless anapole condition without sophisticated manipulation of electromagnetic multipolar moments of all orders to realize superpositions of suppressed moment strengths at the same wavelength. As a result, high contrast reconfigurable optical scattering utilizing the unique combination of structured light and structured Mie resonances can be realized. It means that a Si nanoparticle whose anapole condition is hidden in an electromagnetic multipolar resonance can be selectively accessed as the radiationless condition or resonant scattering state by utilizing different tightly focused CVBs. More importantly, experimental validation based on a simple Si nanodisk in the visible spectrum is provided to further consolidate the proposed reconfigurable optical scattering. Our results might provide a basic idea to realize a reconfigurable electromagnetic atom for meta-optics. By combining both degrees of freedom in structured light and structured Mie resonances, one might anticipate the possibility to realize ultrafast manipulation of optical signal without applying optical nonlinear and optomechanic effects.

References

1. Bohren CF, Huffman DR. *Absorption and Scattering of Light by Small Particles* (John Wiley & Sons, New York, 1983).
2. Kuznetsov AI, Miroshnichenko AE, Fu YH, Zhang JB, Luk'Yanchuk B. Magnetic light. *Sci Rep* **2**, 492 (2012).
3. Krasnok A, Baranov D, Li HN, Miri MA, Monticone F et al. Anomalies in light scattering. *Adv Opt Photonics* **11**, 892–951 (2019).
4. Afanasiev GN, Stepanovsky YP. The electromagnetic field of elementary time-dependent toroidal sources. *J Phys A:Math Gen* **28**, 4565–4580 (1995).
5. Fedotov VA, Rogacheva AV, Savinov V, Tsai DP, Zheludev NI. Resonant transparency and non-trivial non-radiating excitations in toroidal metamaterials. *Sci Rep* **3**, 2967 (2013).
6. Miroshnichenko AE, Evlyukhin AB, Yu YF, Bakker RM, Chipouline A et al. Nonradiating anapole modes in dielectric nanoparticles. *Nat Commun* **6**, 8069 (2015).
7. Gurvitz EA, Ladutenko KS, Dergachev PA, Evlyukhin AB, Miroshnichenko AE et al. The high-order toroidal moments and anapole states in all-dielectric photonics. *Laser Photonics Rev* **13**, 1800266 (2019).
8. Grinblat G, Li Y, Nielsen MP, Oulton RF, Maier SA. Enhanced third harmonic generation in single germanium nanodisks excited at the anapole mode. *Nano Lett* **16**, 4635–4640 (2016).
9. Wei L, Xi Z, Bhattacharya N, Urbach HP. Excitation of the radiationless anapole mode. *Optica* **3**, 799–802 (2016).
10. Nemkov NA, Basharin AA, Fedotov VA. Nonradiating sources, dynamic anapole, and Aharonov-Bohm effect. *Phys Rev B* **95**, 165134 (2017).
11. Zenin VA, Evlyukhin AB, Novikov SM, Yang YQ, Malureanu R et al. Direct amplitude-phase near-field observation of higher-order anapole states. *Nano Lett* **17**, 7152–7159 (2017).
12. Gongora JST, Miroshnichenko AE, Kivshar YS, Fratalocchi A. Anapole nanolasers for mode-locking and ultrafast pulse generation. *Nat Commun* **8**, 15535 (2017).
13. Grinblat G, Li Y, Nielsen MP, Oulton RF, Maier SA. Efficient third harmonic generation and nonlinear subwavelength imaging at a higher-order anapole mode in a single germanium nanodisk. *ACS Nano* **11**, 953–960 (2017).
14. Luk'yanchuk B, Paniagua-Domínguez R, Kuznetsov AI, Miroshnichenko AE, Kivshar YS. Hybrid anapole modes of high-index dielectric nanoparticles. *Phys Rev A* **95**, 063820 (2017).
15. Yang YQ, Zenin VA, Bozhevolnyi SI. Anapole-assisted strong field enhancement in individual all-dielectric nanostructures. *ACS Photonics* **5**, 1960–1966 (2018).
16. Parker JA, Sugimoto H, Coe B, Eggena D, Fujii M et al. Excitation of nonradiating anapoles in dielectric nanospheres. *Phys Rev Lett* **124**, 097402 (2020).
17. Manna U, Sugimoto H, Eggena D, Coe B, Wang R et al. Selective excitation and enhancement of multipolar resonances in dielectric nanospheres using cylindrical vector beams. *J Appl Phys* **127**, 033101 (2020).
18. Zhang TY, Che Y, Chen K, Xu J, Xu Y et al. Anapole mediated giant photothermal nonlinearity in nanostructured silicon. *Nat Commun* **11**, 3027 (2020).
19. Li Y, Huang ZJ, Sui Z, Chen HJ, Zhang XY et al. Optical anapole mode in nanostructured lithium niobate for enhancing second harmonic generation. *Nanophotonics* **9**, 3575–3585 (2020).
20. Sanz-Fernández C, Molezuelas-Ferreras M, Lasa-Alonso J, de Sousa N, Zambrana-Puyalto X et al. Multiple Kerker anapoles in dielectric microspheres. *Laser Photonics Rev* **15**, 2100035 (2021).
21. Luk'yanchuk B, Paniagua-Domínguez R, Kuznetsov AI, Miroshnichenko AE, Kivshar YS. Suppression of scattering for small dielectric particles: anapole mode and invisibility. *Philos Trans R Soc A:Mathemat Phys Eng Sci* **375**, 20160069 (2017).
22. Baryshnikova KV, Smirnova DA, Luk'yanchuk BS, Kivshar YS. Optical anapoles: concepts and applications. *Adv Opt Mater* **7**, 1801350 (2019).
23. Koshelev K, Favraud G, Bogdanov A, Kivshar Y, Fratalocchi A. Nonradiating photonics with resonant dielectric nanostructures. *Nanophotonics* **8**, 725–745 (2019).
24. Yang YQ, Bozhevolnyi SI. Nonradiating anapole states in nanophotonics: from fundamentals to applications. *Nanotechnology* **30**, 204001 (2019).
25. Fang CZ, Yang QY, Yuan QC, Gan XT, Zhao JL et al. High-Q resonances governed by the quasi-bound states in the continuum in all-dielectric metasurfaces. *Opto-Electron Adv* **4**, 200030 (2021).
26. Savinov V, Papasimakis N, Tsai DP, Zheludev NI. Optical anapoles. *Commun Phys* **2**, 69 (2019).
27. Monticone F, Sounas D, Krasnok A, Alù A. Can a nonradiating mode be externally excited? Nonscattering states versus embedded eigenstates. *ACS Photonics* **6**, 3108–3114 (2019).
28. Wu PC, Liao CY, Savinov V, Chung TL, Chen WT et al. Optical anapole metamaterial. *ACS Nano* **12**, 1920–1927 (2018).
29. Youngworth KS, Brown TG. Focusing of high numerical aperture cylindrical-vector beams. *Opt Express* **7**, 77–87 (2000).
30. Zhan QW, Leger JR. Focus shaping using cylindrical vector beams. *Opt Express* **10**, 324–331 (2002).
31. Gu B, Cui YP. Nonparaxial and paraxial focusing of azimuthal-

variant vector beams. *Opt Express* **20**, 17684–17694 (2012).

32. Lou YJ, Fang YS, Ruan ZC. Optical computation of divergence operation for vector fields. *Phys Rev Appl* **14**, 034013 (2020).

33. Xian MC, Xu Y, Ouyang X, Cao YY, Lan S et al. Segmented cylindrical vector beams for massively-encoded optical data storage. *Sci Bull* **65**, 2072–2079 (2020).

34. Das T, Iyer PP, DeCrescent RA, Schuller JA. Beam engineering for selective and enhanced coupling to multipolar resonances. *Phys Rev B* **92**, 241110 (2015).

35. Woźniak P, Banzer P, Leuchs G. Selective switching of individual multipole resonances in single dielectric nanoparticles. *Laser Photonics Rev* **9**, 231–240 (2015).

36. Guclu C, Veysi M, Capolino F. Photoinduced magnetic nanoprobe excited by an azimuthally polarized vector beam. *ACS Photonics* **3**, 2049–2058 (2016).

37. Das T, Schuller JA. Dark modes and field enhancements in dielectric dimers illuminated by cylindrical vector beams. *Phys Rev B* **95**, 201111 (2017).

38. Manna U, Lee JH, Deng TS, Parker J, Shepherd N et al. Selective induction of optical magnetism. *Nano Lett* **17**, 7196–7206 (2017).

39. Deng F, Liu HF, Panmai M, Lan S. Sharp bending and power distribution of a focused radially polarized beam by using silicon nanoparticle dimers. *Opt Express* **26**, 20051–20062 (2018).

40. Klimov V. Manifestation of extremely high-Q pseudo-modes in scattering of a Bessel light beam by a sphere. *Opt Lett* **45**, 4300–4303 (2020).

41. Melik-Gaykazyan EV, Kruk SS, Camacho-Morales R, Xu L, Rahmani M et al. Selective third-harmonic generation by structured light in Mie-resonant nanoparticles. *ACS Photonics* **5**, 728–733 (2018).

42. Koshelev K, Kruk S, Melik-Gaykazyan E, Choi JH, Bogdanov A et al. Subwavelength dielectric resonators for nonlinear nanophotonics. *Science* **367**, 288–292 (2020).

43. Zhan QW. Trapping metallic Rayleigh particles with radial polarization. *Opt Express* **12**, 3377–3382 (2004).

44. Zhang YQ, Shen JF, Min CJ, Jin YF, Jiang YQ et al. Nonlinearity-induced multiplexed optical trapping and manipulation with femtosecond vector beams. *Nano Lett* **18**, 5538–5543 (2018).

45. Liu J, Zheng M, Xiong ZJ, Li ZY. 3D dynamic motion of a dielectric micro-sphere within optical tweezers. *Opto-Electron Adv* **4**, 200015 (2021).

46. Novotny L, Beversluis MR, Youngworth KS, Brown TG. Longitudinal field modes probed by single molecules. *Phys Rev Lett* **86**, 5251–5254 (2001).

47. Bauer T, Orlov S, Peschel U, Banzer P, Leuchs G. Nanointerferometric amplitude and phase reconstruction of tightly focused vector beams. *Nat Photonics* **8**, 23–27 (2014).

48. Feng TH, Xu Y, Zhang W, Miroshnichenko AE. Ideal magnetic dipole scattering. *Phys Rev Lett* **118**, 173901 (2017).

49. Liu W, Zhang JF, Miroshnichenko AE. Toroidal dipole-induced transparency in core−shell nanoparticles. *Laser Photonics Rev* **9**, 564–570 (2015).

50. Papasimakis N, Fedotov VA, Savinov V, Raybould TA, Zheludev NI. Electromagnetic toroidal excitations in matter and free space. *Nat Mater* **15**, 263–271 (2016).

51. Kaelberer T, Fedotov VA, Papasimakis N, Tsai DP, Zheludev NI. Toroidal dipolar response in a metamaterial. *Science* **330**, 1510–1512 (2010).

52. Hoang TX, Chen XD, Sheppard CJR. Multipole theory for tight focusing of polarized light, including radially polarized and other special cases. *J Opt Soc Am A* **29**, 32–43 (2012).

Acknowledgements

Competing interests

The authors declare no competing financial interests.

Supplementary information

Supplementary information for this paper is available at
https://doi.org/10.29026/oea.2022.210014